J. Membrane Biol. 85, 95–109 (1985)

The Journal of
Membrane Biology

Topical Review

Determination of Retinal Chromophore Structure in Bacteriorhodopsin with Resonance Raman Spectroscopy

Steven O. Smith, Johan Lugtenburg*, and Richard A. Mathies
Chemistry Department, University of California, Berkeley, California 94720

Introduction

Bacteriorhodopsin (BR) is a 26,000-dalton intrinsic membrane protein that functions as a light-driven proton pump in the "purple membrane" of *Halobacterium halobium* (Birge, 1981; Stoeckenius & Bogomolni, 1982). Absorption of a photon by the retinal prosthetic group in bacteriorhodopsin initiates the cyclic photochemical reaction shown in Fig. 1, which efficiently transports hydrogen ions across the bacterial cell membrane (Lozier, Bogomolni & Stoeckenius, 1975). The resulting electrochemical proton gradient is coupled to the synthesis of ATP, the transport of amino acids and cations, and may also drive cell locomotion (Racker & Stoeckenius, 1974; Stoeckenius & Bogomolni, 1982). Bacteriorhodopsin's amino acid sequence has been determined (Khorana et al., 1979; Ovchinnikov et al., 1979), and based on low-resolution electron density maps it is believed that the polypeptide spans the membrane in seven α-helical segments (Henderson & Unwin, 1975). The retinal chromophore is located within the hydrophobic interior of the protein (Kouyama, Kinosita & Ikegami, 1983) attached to lysine 216 via a protonated Schiff base linkage (Lewis et al., 1974; Rothschild et al., 1982). Determining the *structure* of the retinal chromophore in BR and its photocycle intermediates is a prerequisite for defining the *functional* role retinal plays in the proton-pumping mechanism.

Resonance Raman spectroscopy can be used as an *in situ* probe of the light-induced structural changes of the retinal chromophore in BR (for reviews, *see* Callender & Honig, 1977; Warshel, 1977; Mathies, 1979). In the resonance Raman experiment, scattering from the chromophore alone can be strongly enhanced by selecting an exciting laser wavelength that lies within the pigment's visible absorption band. The resulting vibrational spectra are highly sensitive to chromophore structure and environment. The Raman spectra shown in Fig. 2 illustrate the dramatic differences which result in both the frequencies and intensities of the chromophore vibrations during the proton-pumping photocycle. These spectra are dominated by an intense ethylenic C=C stretching vibration between 1500 and 1600 cm^{-1}. The C—C single bond stretches and the vinyl hydrogen in-plane rocks appear in the distinctive 1100–1400 cm^{-1} "fingerprint" region. The intensities and frequencies of these modes are sensitive to the *cis-trans* configuration of the C=C double bonds as well as the conformation of the C—C single bonds. Translating these vibrational frequencies and intensities into chromophore structure, however, requires assigning the Raman lines to specific vibrational normal modes.

Early vibrational assignments of the retinal chromophore in bacteriorhodopsin were based on isotopic labeling near the Schiff base and on comparison with retinal model compounds. Lewis et al. (1974) recognized that suspension of purple membrane in D_2O exchanges the Schiff base proton for a deuteron, causing a characteristic shift in the frequency of the C=NH Schiff base stretching vibration. Also, qualitative comparison of Raman spectra of BR_{568} and M_{412} with spectra of retinal Schiff base isomers provided an *in situ* demonstration that the retinal configuration in BR_{568} is all-*trans* and that the configuration in M_{412} is 13-*cis* (Aton et al., 1977; Stockburger et al., 1979; Braiman & Mathies, 1980). These studies also revealed that

Key Words bacteriorhodopsin · resonance Raman · proton-pumping mechanism · retinal isotopic derivatives · vibrational assignments · *cis-trans* isomerization

* *Permanent address:* Chemistry Department, Leiden University, 2300 RA Leiden, The Netherlands.

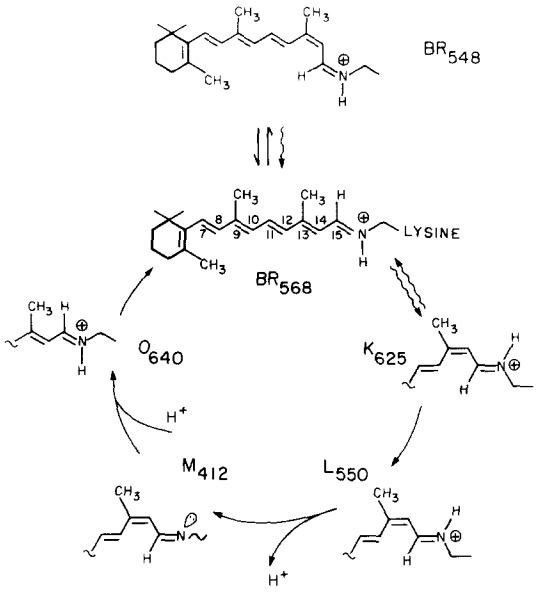

Fig. 1. Photochemical reaction scheme of bacteriorhodopsin, giving the retinal chromophore structure in each intermediate (Smith et al., 1984*a*). The parent pigment, light-adapted bacteriorhodopsin (BR_{568}), contains an all-*trans* retinal chromophore that is attached to lysine 216 through a protonated Schiff base linkage. Photolysis forms the red-absorbing K_{625} intermediate which cycles in ~10 msec back to BR_{568} through L_{550}, M_{412} and O_{640}. Photoisomerization about the C_{13}=C_{14} bond in the $BR_{568} \rightarrow K_{625}$ transition translates the Schiff base proton across the retinal binding site to a new environment storing ~16 kcal/mole of enthalpy (Birge & Cooper, 1983). Subsequent thermal steps channel this energy into proton transport. In the dark, BR_{568} slowly converts to dark-adapted bacteriorhodopsin which contains an approximately equal mixture of all-*trans* and 13-*cis* protonated Schiff base chromophores (denoted BR_{568} and BR_{548}, respectively). Subscripts refer to room temperature absorption maxima, except for the K photoproduct which is most conveniently studied when trapped at low temperature (77°K)

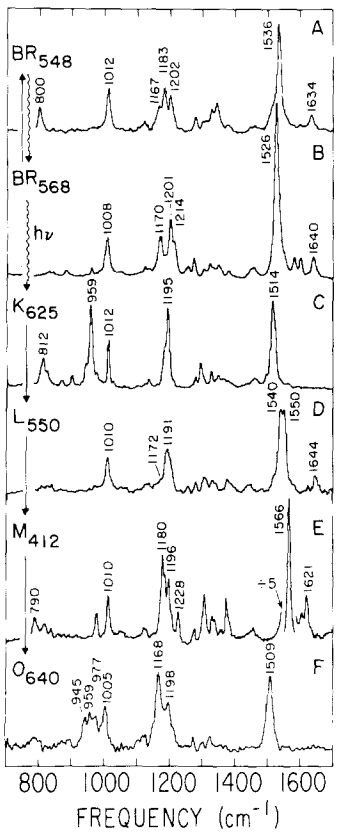

Fig. 2. Resonance Raman spectra of bacteriorhodopsin's photocycle intermediates. Changes in chromophore structure and environment are detected and analyzed through the differences in the vibrational frequencies and intensities, especially in the 1100–1400 cm^{-1} "fingerprint" region. The spectra of BR_{568}, M_{412}, and K_{625} are from Braiman and Mathies (1980, 1982). The BR_{548}, L_{550} and O_{640} spectra are from Smith et al. (1983*a*, 1984*a*). Room-temperature spectra were obtained using purple membrane fragments consisting of ~75% BR and 25% lipid suspended in H_2O buffer. The K_{625} spectra were obtained at 77°K using a purple membrane pellet

protein binding induces significant changes in the vibrational spectrum of the chromophore.

Recent studies using selective isotopic modification of a variety of chromophore positions have demonstrated that quantitative comparison of *specific* chromophore vibrations allows even greater access to the detailed structural information contained in the Raman spectrum. By assigning the Raman bands to specific normal modes in both the retinal model compounds (Curry et al., 1982, 1984; Saito & Tasumi, 1983; Smith et al., 1985) and in the pigments (Massig et al., 1982; Smith et al., 1983*a*, 1984*a*), comparison of vibrational *assignments* can be used as a probe of both chromophore geometry and protein-chromophore interactions.

The first section of this review briefly discusses resonance Raman theory and the methods used to obtain resonance Raman spectra of bacteriorhodopsin. Next we describe how the resonance Raman spectrum can be used to determine the structure of the protein-bound retinal chromophore through the use of selective isotopic substitution. With this background, the spectra of bacteriorhodopsin's photointermediates are analyzed and key chromophore structural features that are involved in proton pumping are discussed.

Methods for Obtaining Resonance Raman Spectra

The basic principles of Raman scattering are illustrated in Fig. 3. A monochromatic laser beam of frequency ν_L, chosen to lie within the electronic absorption band of a chromophore, is focused on the sample, and the frequency and intensity of the *inelastically scattered* light is measured. The *frequency difference* between the incident (ν_L) and

Raman scattered (ν_s) light corresponds to the vibrational frequencies of the chromophore. The advantage of using resonance Raman spectroscopy to study chromophore structure lies in the resonance enhancement effect. As the incident laser frequency approaches the frequency separation between the chromophore's ground and excited electronic states, the cross section for Raman scattering increases, resulting in an enormous enhancement of the scattering intensity in the chromophore's vibrational modes. For example, when excited near 568 nm, the cross section for the 1526 cm^{-1} ethylenic stretching mode of BR_{568} is more than 10^5 times larger than that for the 992 cm^{-1} line in benzene, one of the strongest lines observed from a nonresonant solvent (Myers, Harris & Mathies, 1983). The resulting increase in *sensitivity* permits sample concentrations as low as 10^{-6} M and illuminated sample volumes of only a few microliters. Furthermore, because this enhancement is selective for chromophore modes, it is possible to obtain spectra of a protein-bound chromophore without interference from the more numerous protein vibrations.

Another advantage of resonance enhancement is that the scattering from a particular intermediate can be *selectively* enhanced by using laser excitation at a wavelength where only that intermediate absorbs. For instance, using 412 nm excitation, scattering from the M_{412} intermediate dominates the Raman spectrum even when only 10–20% of the pigment is in the M_{412} form. In practice, the choice of laser wavelength is also governed by laser-induced fluorescence of the sample, as well as absorption overlap with other spectral intermediates. Because large fluorescence backgrounds generated by the incident laser light can mask the relatively weak Raman lines, it is often necessary to select an excitation wavelength such that the Raman spectrum falls outside of the fluorescence band. Furthermore, when the absorption bands of two intermediates overlap, it is desirable to choose a laser wavelength which maximizes the *relative* resonance enhancement of the intermediate of interest.

There are two challenges encountered in performing Raman experiments on retinal-containing pigments. First, the retinal chromophore is photosensitive and absorption of probe laser light can result in photoalteration of the sample as it is being studied. Second, the bacteriorhodopsin intermediates appear with rise times ranging from picoseconds to milliseconds, so that methods must be developed to obtain Raman spectra with varying time resolution. A wide range of novel solutions to these problems have now been developed, and several of the more useful approaches are discussed below.

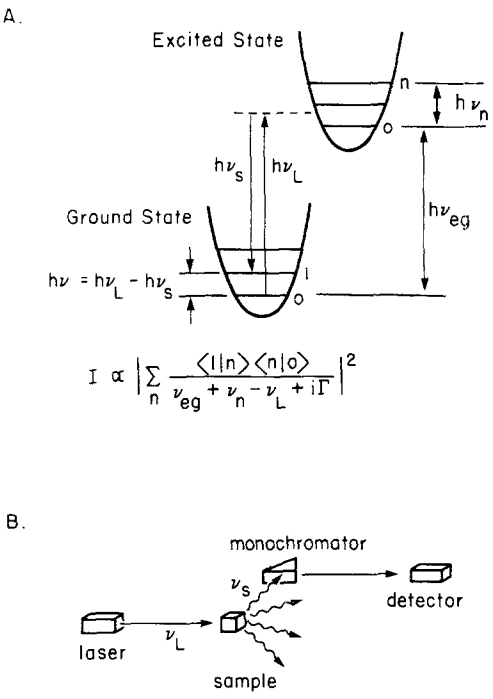

Fig. 3. Schematic of the resonance Raman experiment. In *A* the ground and excited state potential surfaces for one normal coordinate in a molecule are depicted. A laser beam of frequency ν_L irradiates the sample, and the inelastically scattered light, ν_s, leaves the molecule in an excited vibrational level of the ground state. The energy differences between incident and scattered photons yield the vibrational spectrum. As the energy of the laser approaches the energy of a vibronic transition in the molecule ($h\nu_{eg} + h\nu_n$), the denominator in the equation for the Raman intensity approaches zero. This causes a dramatic increase in the intensity or "resonance enhancement" of the vibrational lines. The numerator in the intensity expression contains Franck-Condon factors which are overlap integrals between vibrational wavefunctions on the ground and excited state potential surfaces. In *B* a schematic of the experimental configuration is presented

Rapid-Flow Techniques

Rapid-flow sampling systems, designed to minimize the contribution of photoproducts to the Raman spectrum, were first developed for Raman studies on visual pigments (Callender et al., 1976; Mathies, Oseroff & Stryer, 1976). In the rapid flow experiment, the photosensitive sample is passed through the laser beam in a high-velocity stream so that any photoproducts formed will be swept out of the irradiated volume before they can accumulate to a significant level. The fraction of molecules that photoisomerize while passing through the laser beam is given by the photoalteration parameter (Mathies et al., 1976)

$$F = (3.824 \times 10^{-21}) P\varepsilon\phi/vd$$

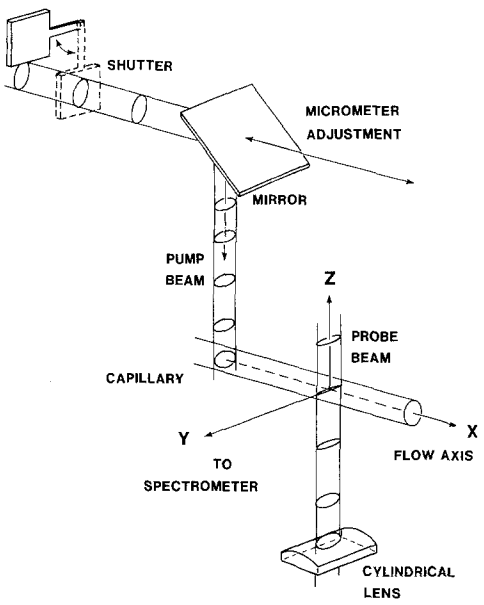

Fig. 4. Dual-beam rapid-flow apparatus for obtaining time-resolved Raman spectra (Smith et al., 1983*a*). Typical flow speeds in a 1.4-mm diameter capillary range from 300 to 500 cm/sec. The time delay (20 μsec – 30 msec) is set by displacing the pump beam ~0.1 to 100 mm upstream from the probe beam with a micrometer. A computer controlled shutter permits the automatic recording of pump-on and pump-off spectra

which depends directly on the laser power (P, photons/sec), the extinction coefficient of the absorbing species at the laser wavelength (ε, M^{-1} cm^{-1}), and the quantum yield for photoreaction (ϕ). F is inversely proportional to the flow velocity (v, cm/sec) and the focused beam diameter (d, cm). To obtain spectra of BR_{568} with a given laser power, the flow rate and beam diameter are simply increased to maintain F less than ~0.1. This means, in essence, that fewer than 10% of the BR molecules photoisomerize while traversing the laser beam. Since the photocycle is complete in ~10 msec, these photolyzed molecules cycle back to BR_{568} long before the recirculating sample returns to the laser beam, so no accumulation of photoproducts occurs.

In many cases, it is necessary to explicitly consider the rate of accumulated photoalteration in the *entire* sample volume. For example, when a small volume of dark-adapted purple membrane is recirculated, even weak laser excitation can "light-adapt" the pigment. This is because the return to the dark-adapted form takes a relatively long time (~20 min) at room temperature. In this circumstance, the photoalteration of the entire volume

$$F_{\text{bulk}} = (3.824 \times 10^{-21})P\phi\varepsilon LT/V$$

can be controlled by decreasing the total irradiation time (T), the path length of the laser beam through the sample (L) and the laser power (P), or by increasing the sample volume (V) (Mathies, 1979). Thus, to obtain spectra of the dark-adapted pigment, large sample volumes and low laser intensities are normally used (*see*, for example: Marcus & Lewis, 1978; Alshuth & Stockburger, 1981).

Time-Resolved Techniques

Time-resolved resonance Raman spectroscopy has been developed extensively by El-Sayed and coworkers who have obtained spectra of bacteriorhodopsin with time resolution from picoseconds to milliseconds (El-Sayed, 1982). For the highest time resolution experiments pulsed lasers are employed, while for microsecond to millisecond experiments flowing samples can be used with continuous wave (cw) lasers. Most experimental designs use a "pump" laser beam to initiate photocycling of BR_{568} and a "probe" laser beam to excite the Raman spectrum. The procedures for attaining time resolution between the pump and probe events, however, differ considerably depending on whether one laser beam (Stockburger et al., 1979; Terner et al., 1979*b*,*c*; Argade & Rothschild, 1983) or two laser beams (Marcus & Lewis, 1978; Braiman & Mathies, 1980; Smith et al., 1983*a*) are used.

Figure 4 depicts a double-beam rapid-flow apparatus used to attain μsec to msec time resolution with cw lasers. The sample is recirculated through a glass capillary and the time resolution between the pump and probe events is controlled by changing the flow rate of the sample and the spatial separation between the two beams. In practice, a *two-color* experiment works best since it allows one to *maximize* resonance enhancement of the intermediate being studied while *minimizing* the contribution of undesired photoproducts to the Raman spectrum. Maximum photocycling is achieved by selecting an intense yellow pump laser that is strongly absorbed by BR_{568} ($F \cong 1$), while the scattering from a particular intermediate is maximized by using a probe beam wavelength that lies within the intermediate's absorption band.

It is also possible to perform experiments with a single cw laser beam. In this case, time resolution is attained by varying the residence time of a flowing sample in the focused laser beam. The single beam serves both to initiate photocycling of the pigment and to excite the Raman spectrum. Spectra of different photocycle intermediates are obtained by increasing the incident laser power and/or changing the flow rate. Because the high-photoalteration

spectra contain scattering from both the intermediates and the unphotolyzed pigment, it is necessary to subtract a low-photoalteration BR_{568} spectrum. There are two drawbacks to the single beam technique. First, it is not possible to optimize both the "pump" and "probe" events. If the laser wavelength is selected to maximize BR_{568} photolysis, resonance enhancement of the intermediate is often reduced relative to BR_{568}. Alternatively, if the laser wavelength is selected to maximize Raman scattering from the intermediate, then the initial photolysis of the BR_{568} pigment is often inefficient. Second, the use of a single *high*-photoalteration laser beam can result in spectra containing a complex mixture of intermediates and their photoproducts. The high-photoalteration spectrum of a particular intermediate has contributions from all intermediates which precede it in the photocycle in addition to contributions from "second order" photoproducts generated when one of these intermediates is photolyzed. Therefore, these single beam experiments are most useful for the early intermediates where the mixture of species formed is simple. For example, Terner et al. (1979*c*) observed scattering from K with time resolution of $\leq$100 nsec by irradiating a rapidly flowing (20 m/sec) purple membrane sample with a tightly focused laser beam.

For nanosecond to picosecond time resolution, pulsed lasers must be employed. Single-pulse 15-nsec and 40-psec experiments have been performed using a cavity-dumped mode-locked dye laser (Hsieh et al., 1981, 1983). However, for the reasons discussed above, a two-pulse sequence from two different lasers is the ideal way to perform fast time-resolved experiments. For example, two-color experiments have been used to obtain the K Raman spectrum with time resolution of 60 nanoseconds (Smith, Braiman & Mathies, 1983*b*). In this case, a 25-nsec pump pulse from a cavity-dumped argon ion laser (514.5 nm) initiates the photochemistry. This is followed by a 25-nsec probe pulse at 647 nm, which excites the K Raman spectrum. The time delay between the pump and probe pulses (60 nsec) determines the time resolution. The advantage of this configuration is that the delay time can be varied independent of the photolysis conditions, although this does require the use of two lasers.

Low-Temperature Techniques

Freezing bacteriorhodopsin at 77°K blocks the thermal decay of the K_{625} intermediate, making it possible to study this primary photoproduct with a static experiment. Photolysis of BR_{568} at this temperature produces a photostationary steady-state mixture of BR_{568} and K_{625} (*see* Fig. 1). Raman spectra of this

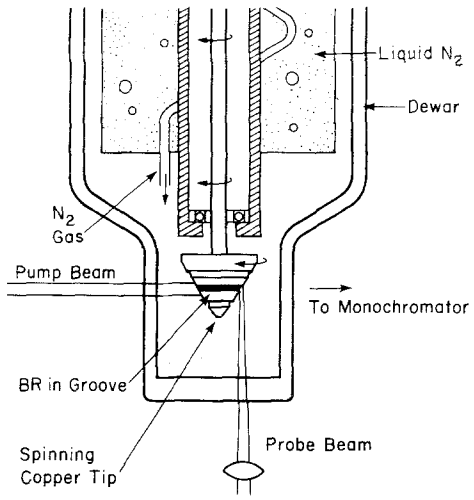

Fig. 5. Low temperature (77°K) spinning cell for obtaining spectra of bacteriorhodopsin (Braiman & Mathies, 1982). The purple membrane sample fills a circular groove in the rotating copper tip. The pump beam illuminates the sample on one side of the spinning cell, producing K_{625} along with BR_{568} fluorescence. The sample is then rotated to the probe beam, which excites the Raman spectrum. This procedure effectively keeps the pump beam-excited fluorescence from being viewed by the detector

mixture are excited with a probe laser wavelength chosen to give maximum resonance enhancement of the K_{625} component. Pure K spectra are then obtained by computer subtraction of the residual BR_{568} scattering. Such low-temperature pump-probe methods were first developed to obtain resonance Raman spectra of the primary photoproduct of rhodopsin (Oseroff & Callender, 1974). In bacteriorhodopsin, however, if the pump and probe beams are coaxial, fluorescence induced by the pump laser can mask the weaker Raman scattering generated by the probe laser. Pande, Callender and Ebrey (1981) avoided high fluorescence backgrounds in their K_{625} spectra by using a probe wavelength on the blue edge of the pump-induced fluorescence (530.9 nm). However, this results in poor resonance enhancement of K_{625} relative to BR_{568}. Braiman and Mathies (1982) reduced the pump-induced fluorescence in their K spectra by using the spinning cell apparatus shown in Fig. 5. Purple membrane is applied to a groove in the conical copper tip which can be cooled to 77°K and spun at 1700 rpm. The key advantage of this approach is that the pump beam, which prepares the photostationary steady state and excites the fluorescence, is spatially displaced from the probe beam. Rotation of the copper tip translates the sample from the pump beam to the probe beam where the K_{625} spectrum is obtained without a high fluorescence background.

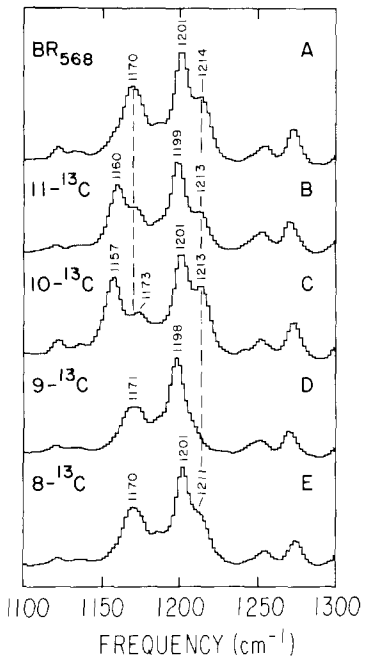

Fig. 6. Resonance Raman spectra of native BR_{568} and its 11-, 10-, 9- and 8- [^{13}C] isotopic derivatives. These spectra illustrate the assignment of the "C_{10}—C_{11}" and "C_8—C_9" single bond stretches at 1170 and 1214 cm^{-1}, respectively

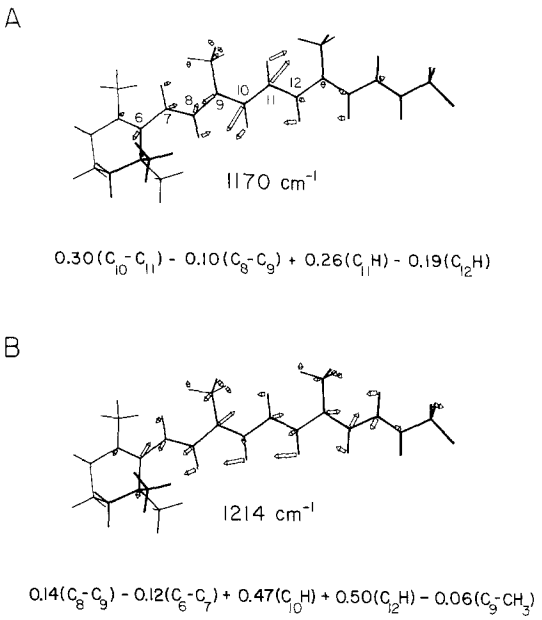

Fig. 7. Mass-weighted atomic displacements and calculated normal mode descriptions for (*A*) the 1170 cm^{-1} "C_{10}—C_{11} stretch" and (*B*) the 1214 cm^{-1} "C_8—C_9 stretch" of BR_{568}. The C_{10}—C_{11} stretching coordinate is the dominant component in the 1170 cm^{-1} mode, while the 1214 cm^{-1} mode is more delocalized with large contributions from C_8—C_9 stretching as well as $C_{10}H$ and $C_{12}H$ rocking motions. Although the hydrogen rocks have significant normal mode coefficients, they are not dominant contributors to the overall potential energy because their reduced mass is $\sim 1/\sqrt{6}$ less than that of the C—C stretches

Methods for Determining Chromophore Structure

To interpret the Raman spectra of bacteriorhodopsin, it is necessary to assign the Raman bands to specific vibrations of the retinal chromophore. Vibrational assignments of the C—C single-bond stretches are made by selective isotopic substitution with ^{13}C, while deuterium substitution of the vinyl hydrogens is used to determine the frequencies of the CCH in-plane rocks and the extent of vibrational *coupling* between the CCH rocks and the C—C stretches. Isotopic derivatives of retinal can be incorporated into bacteriorhodopsin by bleaching the native chromophore with light and hydroxylamine followed by addition of labeled retinal to the apoprotein (Braiman & Mathies, 1980). An alternative, more convenient procedure involves the addition of retinal to bacterio-opsin obtained from a retinal-deficient mutant of *H. halobium* (Smith et al., 1983*a*). These "isomorphous" substitutions provide an excellent probe of the vibrational structure as they do not change the chromophore's structure or interactions with the surrounding protein.

Figure 6 presents an example of how selective ^{13}C-substitution can be used to assign the single-bond stretching modes in BR_{568}. In the native pigment, the C—C stretching region exhibits lines at 1170, 1201 and 1214 cm^{-1}. In the 11-[^{13}C] derivative, the 1170 cm^{-1} line shifts down 10 cm^{-1} to 1160 cm^{-1}, while the frequencies of the other Raman lines are not changed. Similarly, in the 10-[^{13}C] derivative, the 1170 cm^{-1} line shifts 13 cm^{-1} confirming the assignment of this vibration as a localized C_{10}—C_{11} stretch. Figure 7*A* presents the atomic displacements for the 1170 cm^{-1} normal mode. The localized character of the C_{10}—C_{11} stretch is obvious from the large relative displacements of C_{10} and C_{11}. The vinyl hydrogen rocks and other C—C stretches make a much smaller contribution to this normal mode. Figures 6*D* and *E* show that the "C_8—C_9 stretching" mode can be assigned at 1214 cm^{-1} based on an $\sim$16 cm^{-1} shift of this line in the 9-[^{13}C] derivative and a 3 cm^{-1} shift in the 8-[^{13}C] derivative. The difference in sensitivity of this mode to ^{13}C substitution at C_8 and C_9 results from vibrational coupling of the C_8—C_9 stretch with the C_9—CH_3 stretch and the $C_{10}H$ in-plane rock. These coordinates combine in the normal mode to produce much larger motion of C_9 than C_8 and hence the larger ^{13}C-shift (*see* Fig. 7*B*). The large contribution of CCH rocking character to the 1214 cm^{-1} mode is also evident in Fig. 7*B*.

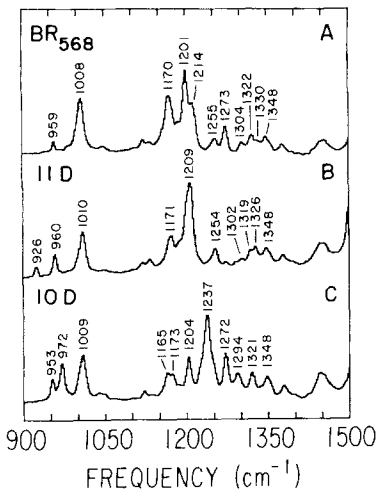

Fig. 8. Resonance Raman spectra of native BR_{568} and its 11D and 10D isotopic derivatives. The $C_{11}H$ rock couples weakly with the C—C stretches, and deuteration produces only minor changes in the vibrational fingerprint. This allows the $C_{11}H$ rocking mode to be assigned at 1273 cm^{-1} based on its disappearance upon 11-deuteration. The $C_{10}H$ rock is strongly coupled with the C—C stretches, and deuteration produces large changes in the fingerprint modes due to a shift of C_8—C_9 stretch character to higher frequency where it mixes strongly with other vibrations

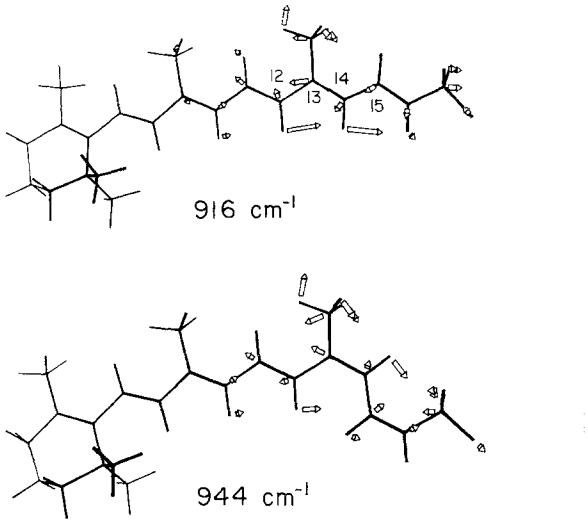

Fig. 9. Mass-weighted atomic displacements for the $C_{12}D$ + $C_{14}D$ rock combination at 916 cm^{-1} in BR_{568} and at 944 cm^{-1} in BR_{548}. The frequency of this highly-localized normal mode is characteristic of the C_{13}=C_{14} configuration. A low frequency (901–916 cm^{-1}) indicates a *trans* configuration, while a high frequency (936–953 cm^{-1}) is diagnostic of a 13-*cis* configuration

The extent of coupling between the C—C stretches and CCH rocks can be determined by selective deuteration of the vinyl hydrogens. When a vinyl hydrogen in-plane rock and a C—C stretch are *coupled*, the resulting normal modes exchange character and "split apart" in frequency. The higher frequency CCH rocking mode gains C—C stretching character and its frequency is raised, while the lower frequency C—C stretching mode gains CCH rocking character and its frequency is lowered. Deuteration eliminates this coupling by lowering the frequency of the CCH rocking vibration from ~1300 to ~970 cm^{-1}, resulting in a frequency increase of the C—C stretch. Figure 8 illustrates the difference in coupling patterns of the $C_{11}H$ and $C_{10}H$ rocks in BR_{568}. The $C_{11}H$ rock is not strongly coupled to any of the C—C stretches, so that 11-deuteration causes only minor changes in the fingerprint region other than the disappearance of the 1273 cm^{-1} $C_{11}H$ rock. In contrast, the $C_{10}H$ rock is strongly coupled with the C_8—C_9 stretch (*see* Fig. 7*B*) so that deuteration at C_{10} produces large changes in both the frequency and intensity of the fingerprint modes. These changes result primarily from a shift of C_8—C_9 character into the 1237 and 1294 cm^{-1} modes. The differences in rock-stretch coupling illustrated here are particularly important when they can be directly related to changes in chromophore structure.

The configurations about the C_{13}=C_{14}, C_{14}—C_{15}, and C=N bonds are of mechanistic importance in the bacteriorhodopsin chromophore. Methods for determining the structure about these bonds will now be presented.

C_{13}=C_{14} Configuration

The configuration about the C_{13}=C_{14} bond in bacteriorhodopsin's intermediates can be determined from differences in vibrational coupling between the internal coordinates localized near the C_{13}=C_{14} bond. Deuteration of C_{15} was the first isotopic modification used to show empirically that characteristic shifts occur in the Raman spectra of 13-*cis* and all-*trans* Schiff base model compounds (Braiman & Mathies, 1980). Subsequent vibrational analysis of all-*trans* and 13-*cis* retinal (Curry et al., 1984) has shown in addition that the in-plane rocking vibrations of the $C_{12}H$ and $C_{14}H$ hydrogens are sensitive to C_{13}=C_{14} configuration. The characteristic dependence of these frequencies on C_{13}=C_{14} configuration is most apparent when the C_{12} and C_{14} positions are deuterated. The deuterated rocking vibrations are then shifted into the 900–1050 cm^{-1} range, where they are easy to assign and interpret because of their relative isolation from C—C stretches and other CCH rocks. The $C_{12}D$ and $C_{14}D$ rocks couple with one another to form an in-phase combination at ~910 cm^{-1} in 13-*trans* chromophores, while in 13-*cis* chromophores the in-phase combination is at ~940 cm^{-1} (*see* Fig. 9). The Table presents the $C_{12}D$

Table. Marker bands for $C_{13}=C_{14}$ configuration using 12,14-D_2 retinal derivatives

	$C_{12}D + C_{14}D$ rock frequency	
Molecule	13-*trans*	13-*cis*
All-*trans* retinal	901	
All-*trans* PSB	909	
13-*cis* retinal		936
13-*cis* PSB		940
BR_{548}		944
BR_{568}	916	
K_{625}		941
L_{550}		953
M_{412}		943
O_{640}	914	

The all-*trans* and 13-*cis* retinal data are from Curry et al. (1984). The BR_{568}, BR_{548} and O_{640} data are from Smith et al. (1983*a*), the K_{625} and L_{550} data are from Smith et al. (1984*a*), and the M_{412} data are from Braiman (1983).

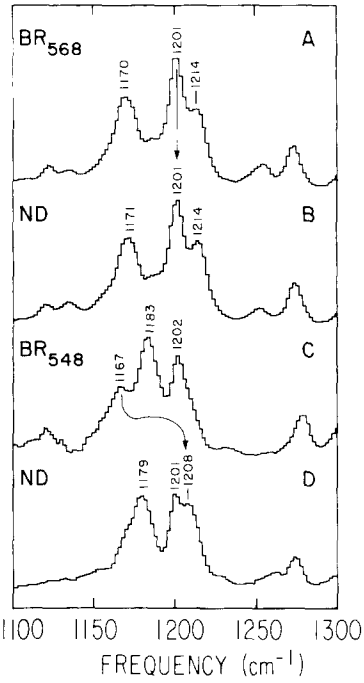

Fig. 10. Determination of C=N configuration. In BR_{568}, the insensitivity of the 1201 cm^{-1} C_{14}—C_{15} stretch to N-deuteration demonstrates that its C=N configuration is *trans*. In BR_{548} the dramatic shift of the 1167 cm^{-1} C_{14}—C_{15} stretch upon suspension in D_2O shows that the C=N configuration in this intermediate is *cis*

+ $C_{14}D$ frequencies for retinal, its protonated Schiff base (PSB), and the BR intermediates. It is evident that *the frequency of the $C_{12}D + C_{14}D$ rock provides an excellent marker band for $C_{13}=C_{14}$ configuration, regardless of the nature of the end group.*

C=N Configuration

The configuration about the Schiff base bond is important in determining the location and displacement of the Schiff base proton during the BR photocycle. This bond is difficult to examine by chemical extraction techniques (Pettei et al., 1977; Tsuda et al., 1980) because they must break the Schiff base bond in the course of the analysis. However, this question can be addressed with the *in situ* Raman technique. Due to the common atom involved in the C_{14}—C_{15} stretch and the $C_{15}NH$ rock, these coordinates are kinetically coupled. This coupling is drastically different for C=N *cis* and C=N *trans* molecules (Smith et al., 1984*a*). In the C=N *cis* configuration the rock-stretch coupling is large, resulting in a 40–60 cm^{-1} shift of the C_{14}—C_{15} stretch upon deuteration of the Schiff base nitrogen. However, in the C=N *trans* configuration, the rock-stretch coupling is small, producing only a slight ($\leq$5 cm^{-1}) shift of the C_{14}—C_{15} stretch upon N-deuteration. Figure 10 illustrates the determination of the C=N configuration in BR_{568} and BR_{548}. The frequency of the 1201 cm^{-1} C_{14}—C_{15} stretch in BR_{568} is not changed upon N-deuteration. This is characteristic of a *trans* C=N bond. However, the 1167 cm^{-1} C_{14}—C_{15} stretch of BR_{548} shifts 41 cm^{-1} to 1208 cm^{-1} in the ND derivative, characteristic of a *cis* C=N bond. It is evident that deuteration of the Schiff base is an effective method for studying the C=N geometry in protonated Schiff bases.

C_{14}—C_{15} Conformation

The low energy barrier for isomerization about C—C single bonds raises the attractive possibility that single-bond isomerizations occur in the BR photocycle. Schulten has proposed that, in addition to the usual $C_{13}=C_{14}$ isomerization, the C_{14}—C_{15} bond undergoes an *s-trans* $\rightarrow$ *s-cis* isomerization in the $BR_{568} \rightarrow K_{625}$ transition generating a 13-*cis*, 14-*s-cis* intermediate (Schulten & Tavan, 1978; Orlandi & Schulten, 1979). Reisomerization of the C_{14}—C_{15} bond would then be triggered by deprotonation of the Schiff base nitrogen during the formation of M_{412}, which could play a key role in the pump mechanism. The development of a method for determining single-bond conformation is therefore of importance.

Vibrational analysis of *s-cis* and *s-trans* butadiene (Curry, 1983) shows that the central C—C stretch is 50–100 cm^{-1} lower in frequency in the

s-cis conformer due to altered kinetic interactions of the C—C stretch with bends of a *cis* polyene. Calculations support the application of these results to the C_{14}—C_{15} bond. Using a force field adapted from the retinal protonated Schiff bases (Smith et al., 1985), the C_{14}—C_{15} stretch is predicted to be 69 cm^{-1} lower in the *s-cis* conformer than in the *s-trans* conformer (Fig. 11). This argues that the *frequency* of the C_{14}—C_{15} stretching mode is sensitive to the C_{14}—C_{15} conformation. This difference between the *s-cis* and *s-trans* conformers results from the difference in coupling between the C_{14}—C_{15} stretch and the $C_{13}C_{14}C_{15}$ and $C_{14}C_{15}N$ bends due to changes in C_{14}—C_{15} *geometry* and thus should be a reliable diagnostic tool. To establish the conformation about the C_{14}—C_{15} bond, it is necessary to determine the frequency of C_{14}—C_{15} stretching coordinate in an intermediate and compare this with the frequency of the C_{14}—C_{15} stretch in the appropriate retinal Schiff base model compound.

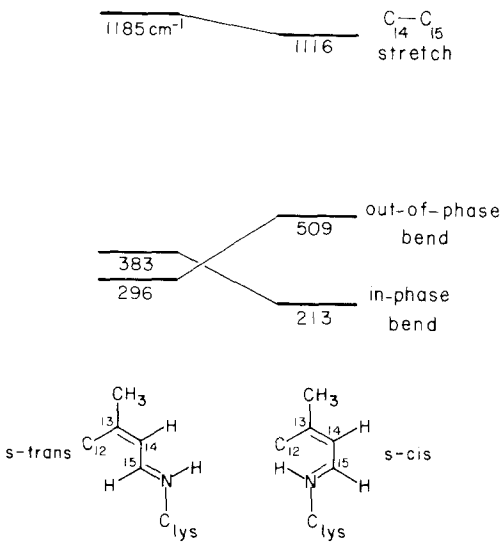

Fig. 11. Calculated vibrational frequencies for planar C_{14}—C_{15} *s-trans* and *s-cis* Schiff base fragments. In the *s-trans* conformer, the in-phase combination of the $C_{13}C_{14}C_{15}$ and $C_{14}C_{15}N$ bends at 383 cm^{-1} couples strongly with the C_{14}—C_{15} stretch and raises its frequency to 1185 cm^{-1}. However, in the *s-cis* conformer the symmetric combination is lowered, reducing the stretch-bend interaction, and the C_{14}—C_{15} stretch drops to 1116 cm^{-1}. The out-of-phase bend is unable to couple with the C_{14}—C_{15} stretch and thus has no effect on the C—C stretch frequency. These frequencies and coupling patterns are based on those observed in *s-cis* and *s-trans* butadiene (Curry, 1983)

Structural Conclusions about the Retinal Chromophore in Bacteriorhodopsin

Light-induced structural changes in bacteriorhodopsin's retinal chromophore drive the translocation of hydrogen ions across the bacterial cell membrane. Vibrational studies of the bacteriorhodopsin intermediates have begun to characterize these reactions and determine the *mechanism* by which the chromophore directs vectorial motion of protons through the interior of the protein. Some of the conclusions relating the structure of the retinal chromophore in the BR intermediates to the proton-pumping mechanism are discussed below.

BR_{568}

Resonance Raman, NMR, and chemical extraction studies have all contributed to showing that the chromophore in BR_{568} is a C_{13}=C_{14} *trans*, C_{15}=NH *trans* protonated Schiff base (Lewis et al., 1974; Aton et al., 1977; Pettei et al., 1977; Braiman & Mathies, 1980; Tsuda et al., 1980; Harbison et al., 1983, 1984; Smith et al., 1984*a*). However, the Raman spectrum of BR_{568} is significantly different from that of the all-*trans* retinal protonated Schiff base (PSB). Figure 12 compares the vibrational assignments of the C—C stretching modes in all-*trans* retinal, the all-*trans* unprotonated and protonated Schiff bases, and BR_{568} (Curry et al., 1982; Smith et al., 1985). The correlation diagram suggests that the differences between the PSB and BR_{568} result from increased delocalization of the conjugated π-system upon binding to the protein (Smith et al., 1985). As the π-electrons become more delocalized, the C—C single-bond stretches gain more "double-bond character" and shift to higher frequency. For instance, protonation of the Schiff base nitrogen causes an increase in π-electron delocalization, which is greatest near the Schiff base and decreases toward the ionone ring. By comparing the Schiff base and the protonated Schiff base spectra (Fig. 12), we see that there is a large shift of the C_{14}—C_{15} (16–38 cm^{-1}) and C_{12}—C_{13} (15 cm^{-1}) stretches and a modest shift of the C_{10}—C_{11} (6–16 cm^{-1}) and C_8—C_9 (8 cm^{-1}) stretches. Placing the PSB into bacterio-opsin shifts each of these C—C stretches up an additional 10 cm^{-1}. The observation that the C_{14}—C_{15} stretch *increases* in frequency in BR_{568} relative to the PSB argues that the C_{14}—C_{15} conformation in the protein is *s-trans*. If BR_{568} were C_{14}—C_{15} *cis*, then the C_{14}—C_{15} stretch would be *reduced* in frequency by more than 50 cm^{-1}. In addition, the similar shifts and frequency ordering and spacing of the C_8—C_9, C_{10}—C_{11}, C_{12}—C_{13} and C_{14}—C_{15} stretches suggests that no strong local protein-chromophore perturbations exist in the C_8—C_{15} region of the chromophore. This is consistent with the point-charge

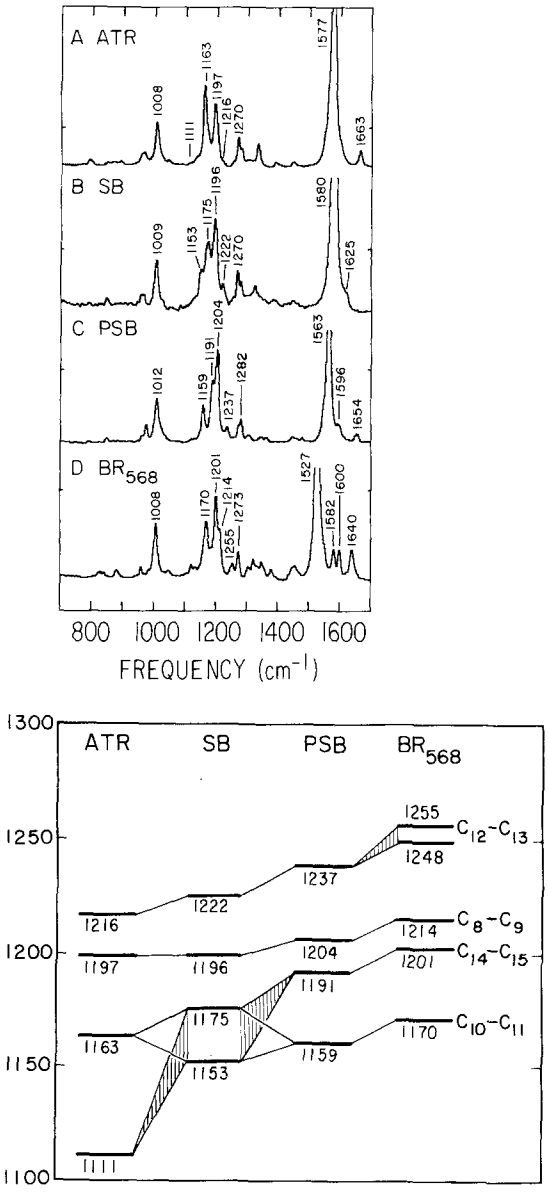

Fig. 12. Resonance Raman spectra and C—C frequency correlations for all-*trans* retinal, its unprotonated and protonated Schiff bases, and BR_{568}. The most dramatic effect of Schiff base formation is the shift of the C_{14}—C_{15} stretch to ~1163 cm^{-1} where it couples with the C_{10}—C_{11} stretch (indicated by cross-hatching) forming two nearly equally mixed modes at 1153 and 1175 cm^{-1}. Protonation of the Schiff base results in an additional ~10 cm^{-1} increase of the C—C stretches due to the more delocalized electronic structure. Incorporation of the all-*trans* PSB into bacterioopsin shifts each C—C stretching frequency ~10 cm^{-1} higher in frequency as a result of even greater electron delocalization. [Reproduced from Smith et al., *Biophys. J.*, 1985, (*in press*) by copyright permission of the Biophysical Society]

model, which argues that the chromophore in BR_{568} interacts with a negative protein residue near the ionone ring (Nakanishi et al., 1980).

Recent resonance Raman experiments by Hildebrandt and Stockburger (1984) have examined the environment of the Schiff base in BR_{568}. They argue, based on a detailed linewidth analysis, that the positively charged Schiff base nitrogen and its negative protein counterion are stabilized by surrounding water molecules. They also observe a line which they assign as the Schiff base N—H stretch at a frequency (3379 cm^{-1}) characteristic of a weakly hydrogen-bonded proton. These observations may help to explain the reduced coupling between the N—H rock and the C=N stretch which causes the low C=N stretching frequency in BR_{568} (Kakitani et al., 1983).

BR_{548}

In the dark, BR_{568} slowly converts to dark-adapted bacteriorhodopsin, which contains an approximately equal mixture of all-*trans* and 13-*cis* protonated Schiff base chromophores (Maeda, Iwasa & Yoshizawa, 1977; Sperling et al., 1977). The all-*trans* component of dark-adapted BR is generally accepted to be identical with BR_{568}, while the 13-*cis* component represents a distinct spectral species called BR_{548}. Interest in the dark conversion of BR_{568} to BR_{548} has arisen for two reasons. First, dark equilibration of all-*trans* and 13-*cis* isomers requires a protein-induced lowering of the thermal barrier for isomerization about the C_{13}=C_{14} bond. It would be useful to know how this is done since protein-catalyzed 13-*cis* → 13-*trans* isomerization plays an important role in the dark conversion of M_{412} back to BR_{568}. Second, the dark-adapted 13-*cis* pigment does not pump protons although it does photocycle. The structural reason for the lack of proton pumping and the physiological relevance of dark-adaptation are unknown.

The resonance Raman spectrum of BR_{548} is obtained by subtracting a BR_{568} spectrum from dark-adapted BR (Marcus & Lewis, 1978; Stockburger et al., 1979; Terner et al., 1979*b*). It is generally accepted that the C_{13}=C_{14} configuration is *cis*, and this is strongly supported by the 944 cm^{-1} $C_{12}D$ + $C_{14}D$ frequency. Also, the N-deuteration studies discussed earlier (Fig. 10) clearly show that the C=N configuration is also *cis* (Smith et al., 1984*a*). This conclusion is fully supported by independent solid-state NMR studies (Harbison et al., 1984). The distinctive pattern of vibrational frequencies and intensities observed in the BR_{548} fingerprint region results in part from the lower frequency of the 1167 cm^{-1} C_{14}—C_{15} stretch compared to the 1201 cm^{-1} C_{14}—C_{15} stretching mode in BR_{568} (*see* Fig. 10; Smith et al., 1983*a*, 1984*a*). The reduced C_{14}—C_{15} stretch frequency in BR_{548} is consistent with the arguments of Curry et al. (1984) that a

C—C single-bond stretch adjacent to a *cis* double bond should be lowered in frequency due to decreased kinetic interaction with the associated skeletal bends. In fact, the C_{14}—C_{15} stretching mode in BR_{548} is 9 cm^{-1} lower in frequency than in the 13-*cis* PSB (1176 cm^{-1}) (Smith, 1985). This is initially surprising since we saw above that protein binding results in a general frequency *increase* of ~10 cm^{-1}. However, in BR_{548} the C_{14}—C_{15} stretch is adjacent to *two cis* double bonds, the C_{13}=C_{14} and C=N, accounting for the additional frequency decrease of the C_{14}—C_{15} stretch.

In summary, dark-adaptation involves a concerted thermal "bicycle pedal" isomerization about both the C_{13}=C_{14} and C=N double bonds, which leaves the Schiff base proton in the same orientation as in BR_{568} (*see* Fig. 1). This is in agreement with the earlier proposal by Orlandi and Schulten (1979), who argued that the energy barrier for the concerted isomerization could be crossed thermally by a *protonated* retinal Schiff base. This suggests that the inability of BR_{548} to pump protons is caused by the presence of the *cis* C=N bond which gives the chromophore an incorrect N—H orientation during photoreaction of the BR_{548} pigment.

K_{625}

The primary photoproduct K_{625} is a key intermediate in proton translocation. Light energy absorbed by BR_{568} is stored in K_{625}, and used to drive the thermal reactions of the photocycle (Birge & Cooper, 1983). Resonance Raman spectra of the K intermediate have been obtained in a photostationary steady state at 77°K (Pande et al., 1981; Braiman & Mathies, 1982) and with picosecond (Hsieh et al., 1981, 1983) and nanosecond (Terner et al., 1979*c*; Smith et al., 1983*b*) time-resolution at room temperature. In addition, excellent Fourier transform infrared (FTIR) difference spectra have been obtained of the $BR_{568} \rightarrow K_{625}$ transition (Bagley et al., 1982; Rothschild & Marrero, 1982; Siebert & Maentele, 1983). It is worth noting that these K_{625} FTIR spectra are very similar to the K Raman data obtained using the low-temperature spinning cell technique (Rothschild et al., 1984*a*). There are three features of the K_{625} spectrum which provide information about energy storage and proton transport: (1) the intense hydrogen out-of-plane wagging vibrations between 800 and 1000 cm^{-1}, (2) the low frequency of the C=N stretching mode and its shift upon N-deuteration, and (3) the high frequency of the C_{14}—C_{15} stretching mode.

Raman spectra obtained at 77°K by Braiman and Mathies (1982) using a 15D-labeled bacteriorhodopsin derivative suggest that the C_{13}=C_{14} configuration in K_{625} is *cis*. This is strongly supported by the observation of a 941 cm^{-1} $C_{12}D + C_{14}D$ rocking vibration. They also observed intense Raman lines in the 800–1000 cm^{-1} region of the spectrum which were assigned as out-of-plane wagging vibrations of the retinal vinyl hydrogens. These modes are expected to have little or no intensity in the Raman spectrum of a planar retinal chromophore, but can be strongly enhanced when the chromophore is conformationally distorted (Eyring et al., 1980; Warshel & Barboy, 1982). Intense hydrogen out-of-plane modes presumably occur in K_{625} because the isomerizing chromophore "runs into" protein residues in the retinal binding site and cannot relax to a planar structure.

Energy storage in the K intermediate is hypothesized to result from isomerization-induced charge separation between the positively charged Schiff base nitrogen and a negatively charged protein counterion (Honig et al., 1979; Warshel, 1979). The validity of this hypothesis can be tested by determining the C=N configuration in K. The insensitivity of the C—C stretches in K_{625} to N-deuteration argues that the C=N configuration is *trans* (Smith et al., 1984*a*). Thus the $BR_{568} \rightarrow K_{625}$ transition involves a single isomerization about the C_{13}=C_{14} bond which must translate the Schiff base proton into a *different* protein environment (*see* Fig. 1). This provides direct experimental evidence for charge separation in the primary photochemical event.

To probe the Schiff base environment in K, vibrational studies have focused on the frequency and isotopic shifts of the Schiff base vibration. The C=N stretching mode in the room temperature Raman spectrum of K was initially assigned at 1626 cm^{-1} based on a shift of 10 cm^{-1} upon N-deuteration (Terner et al., 1979*c*). Subsequent $BR_{568} - K_{625}$ difference spectra at 77°K have shown that the ~1623 cm^{-1} line is insensitive to deuteration, but that a line at 1608 cm^{-1} shifts in D_2O (Bagley et al., 1982; Rothschild & Marrero, 1982; Siebert & Maentele, 1983). FTIR results using 10-[^{13}C]-labeled bacteriorhodopsin have more clearly established that the 1608 cm^{-1} line at low temperature is the Schiff base mode (Rothschild et al., 1984*b*). A C=N stretching mode at or below 1620 cm^{-1} is unusually low for a protonated Schiff base vibration and would be more characteristic of an unprotonated Schiff base. However, it seems clear that K_{625} is protonated based on its red-shifted absorption band and the sensitivity of other K_{625} vibrational lines to suspension in D_2O (Bagley et al., 1982). A low C=NH frequency could result from increased π-electron delocalization in K due to displacement of the Schiff base from its protein coun-

terion. A more detailed characterization of the Schiff base mode in K at low temperature and at ambient temperature will be important because this vibration should provide information about changes in the hydrogen-bonding of the Schiff base proton.

The assignment of the C_{14}—C_{15} stretch in K_{625} is important for determining the C_{14}—C_{15} conformation. ^{13}C-substitution of the K_{625} chromophore at C_{14} and C_{15} results in a 6 cm^{-1} shift of the 1195 cm^{-1} fingerprint line (Smith et al., 1984*a*). Furthermore, deuteration at C_{15} shifts the 1195 cm^{-1} line to 1191 cm^{-1} and increases intensity at 1224 cm^{-1} (Braiman & Mathies, 1982). These results indicate that the C_{14}—C_{15} stretch contributes significantly to the intense 1195 cm^{-1} line in the native K spectrum which is ~20 cm^{-1} *above* the C_{14}—C_{15} stretch in the 13-*cis* protonated Schiff base. This suggests that the conformation about the C_{14}—C_{15} bond in K is *s-trans*. If K_{625} had an *s-cis* geometry, its C_{14}—C_{15} stretch would be expected at a significantly lower frequency than in the 13-*cis*, 14-*s-trans* protonated Schiff base. It must be noted, however, that the C_{14}—C_{15} bond order and thus the C_{14}—C_{15} frequency would be expected to increase in K as a result of π-electron delocalization and might cancel out the direct effects of a *cis* single bond. Comparison of the all-*trans* PSB with BR_{568} shows that protein-induced electron delocalization, which results in a shift of the absorption maximum from 440 to 568 nm, is correlated with only a 10 cm^{-1} frequency shift of the C_{14}—C_{15} stretch. When this correlation is applied to K (λ_{max} = 625), the predicted upshift (15 cm^{-1}) is clearly not large enough to counteract the $\geq$50 cm^{-1} frequency reduction expected for *s-cis* isomerization. The conclusion that K_{625} is C_{14}—C_{15} *s-trans* is consistent with the model of Schulten and Tavan (1978) which predicts isomerization from C_{13}=C_{14} *trans*, C_{14}—C_{15} *trans* to C_{13}=C_{14} *cis*, C_{14}—C_{15} *cis* in the $BR_{568} \rightarrow K_{625}$ transition.

L_{550}

The L_{550} intermediate is formed by relaxation of the torsionally distorted primary photoproduct. Both low temperature (Narva, Callender & Ebrey, 1981) and room temperature (Marcus & Lewis, 1978; Stockburger et al., 1979; Terner et al., 1979*b*; Argade & Rothschild, 1983; Smith et al., 1984*a*) L_{550} resonance Raman spectra have been obtained. The configuration about the C_{13}=C_{14} bond in L_{550} has been assumed to be *cis* since both K_{625} and M_{412} have 13-*cis* chromophores. Direct *in-situ* evidence for the configuration about the C_{13}=C_{14} bond in L_{550} comes from the frequency of the $C_{12}D$ + $C_{14}D$ in-plane rock in the 12,14-D_2 derivative. The observation of a line at 953 cm^{-1} demonstrates that L_{550} is 13-*cis*. Furthermore, deuteration of the Schiff base has been used to show that the C=N configuration in L_{550} is *trans* (Smith et al., 1984*a*). Finally, the assignment of the C_{14}—C_{15} stretching mode at 1172 cm^{-1}, very close to its frequency in the 13-*cis* PSB, argues that the C_{14}—C_{15} conformation is *s-trans*. Thus, the structural assignments in L_{550} agree with the idea that the $K_{625} \rightarrow L_{550}$ transition results from a simple relaxation about slightly distorted C—C single bonds. The model of Schulten and Tavan (1978) agrees with the conclusion that the $K_{625} \rightarrow L_{550}$ transition does not involve any formal isomerizations, although it incorrectly predicts that the C_{14}—C_{15} conformation in L_{550} is *s-cis*.

One striking feature of the L_{550} Raman spectrum is the presence of two ethylenic stretching vibrations at 1540 and 1550 cm^{-1}. Although the retinal chromophore contains *five* ethylenic stretching fundamentals, only one mode typically has the correct in-phase combination of the individual C=C stretches to be observed with significant intensity. Marcus and Lewis (1978) attempted to account for the second intense C=C stretching mode in the L_{550} spectrum by proposing that an additional intermediate, *X*, occurred between L_{550} and M_{412}, although no such intermediate has been observed in kinetic absorption spectra. Argade and Rothschild (1983) addressed the possibility that a photoproduct of L_{550} is responsible for the second intense ethylenic line by carefully measuring the relative intensities of the two ethylenic bands as a function of incident laser power and exposure times. They observed no differences between the low- and high-photoalteration spectra, suggesting that the two lines result from a single L_{550} species. Furthermore, the similar relative intensities of the two ethylenic bands at different time points during the photocycle argues that the $L \rightarrow X \rightarrow M$ scheme proposed by Marcus and Lewis is incorrect.

The conversion of L_{550} to M_{412} involves deprotonation of the Schiff base nitrogen. Such a transition presumably results from a change in the pK_a of the Schiff base proton due to a change in the Schiff base environment. Deprotonation of a tyrosine residue has been observed during the decay of L_{550} to M_{412} (Bogomolni, Stubbs & Lanyi, 1978; Hanamoto, Dupis & El-Sayed, 1984) which raises the intriguing possibility that the second intense ethylenic line in the L_{550} spectrum may be due to a second L species with an altered *protein* environment. Additional studies are needed to establish whether the L_{550} spectrum results from a single molecular species or from two components in rapid *thermal* equilibrium.

M_{412}

Deprotonation of the Schiff base nitrogen in the formation of M_{412} transfers a proton to a protein residue on one side of the retinal binding pocket. For proton transfer to occur in only one direction across the cell membrane, it seems likely that the Schiff base in M_{412} *reprotonates* by accepting a proton from a *different* protein residue. Models in which the M_{412} intermediate serves as a unidirectional "gate" for proton transfer postulate either isomerization about the C_{14}—C_{15} bond (Schulten & Tavan, 1978) or configurational changes about the C=N bond (Braiman, 1983) before reprotonation. The observation that M_{412} decay is biphasic suggests the presence of two intermediates (Slifkin & Caplan, 1975; Hess & Kuschmitz, 1977; Li, Govindjee & Ebrey, 1984), which may differ in C_{14}—C_{15} conformation or C=N configuration.

Resonance Raman spectra of M_{412} have been obtained at high pH (Aton et al., 1977) where the M intermediate accumulates, and at pH 7 using time-resolved techniques (Terner, Campion & El-Sayed, 1977; Marcus & Lewis, 1978; Stockburger et al., 1979; Braiman & Mathies, 1980). These spectra have established that the chromophore is a 13-*cis* unprotonated Schiff base (*see also* the 12,14-D_2 Table). However, the C=N configuration has not been determined because the vibrational coupling method discussed previously requires that the Schiff base be protonated. Also, the C_{14}—C_{15} conformation in M_{412} is unknown. These will obviously be key areas for future experiments.

O_{640}

Formation of O_{640}, the principal intermediate in the $M_{412} \rightarrow BR_{568}$ conversion, is kinetically associated with the uptake of protons by the cell membrane (Lozier et al., 1975), and its subsequent decay completes the BR photocycle. Thus, the structural changes in the formation and decay of the O_{640} intermediate are important in "resetting" the proton-pumping mechanism. The isotopic shifts observed in the 15D and 12,14-D_2 O_{640} spectra demonstrate that O_{640} has an all-*trans* Schiff base chromophore (Smith et al., 1983*a*), while the shift of the C=N stretching mode in D_2O shows that the Schiff base nitrogen is protonated (Terner et al., 1979*a*; Smith et al., 1983*a*). Furthermore, the insensitivity of the fingerprint modes to N-deuteration argues that the C=N bond has a *trans* configuration. Thus, the conversion of M_{412} to O_{640} involves both C_{13}=C_{14} isomerization and Schiff base protonation. The mechanism through which this occurs is unclear. Since the energy barrier for thermal isomerization about C=C double bonds is much lower for protonated than for unprotonated Schiff bases (Orlandi & Schulten, 1979), protonation would be expected to precede (and catalyze?) isomerization in the $M_{412} \rightarrow O_{640}$ transition. Experiments looking for a protonated 13-*cis* chomophore between M_{412} and O_{640} (N_{520}?; Lozier et al., 1975) may prove fruitful.

Summary

The analysis of the vibrational spectrum of the retinal chromophore in bacteriorhodopsin with isotopic derivatives provides a powerful "structural dictionary" for the translation of vibrational frequencies and intensities into structural information. Of importance for the proton-pumping mechanism is the unambiguous determination of the configuration about the C_{13}=C_{14} and C=N bonds, and the protonation state of the Schiff base nitrogen. Vibrational studies have shown that in light-adapted BR_{568} the Schiff base nitrogen is protonated and both the C_{13}=C_{14} and C=N bonds are in a *trans* geometry. The formation of K_{625} involves the photochemical isomerization about only the C_{13}=C_{14} bond which displaces the Schiff base proton into a different protein environment. Subsequent Schiff base deprotonation produces the M_{412} intermediate. Thermal reisomerization of the C_{13}=C_{14} bond and reprotonation of the Schiff base occur in the $M_{412} \rightarrow O_{640}$ transition, resetting the proton-pumping mechanism. The vibrational spectra can also be used to examine the conformation about the C—C single bonds. The frequency of the C_{14}—C_{15} stretching vibration in BR_{568}, K_{625}, L_{550} and O_{640} argues that the C_{14}—C_{15} conformation in these intermediates is *s-trans*.

Conformational distortions of the chromophore have been identified in K_{625} and O_{640} through the observation of intense hydrogen out-of-plane wagging vibrations in the Raman spectra (*see* Fig. 2). These two intermediates are the direct products of chromophore isomerization. Thus it appears that following isomerization in a tight protein binding pocket, the chromophore cannot easily relax to a planar geometry. The analogous observation of intense hydrogen out-of-plane modes in the primary photoproduct in vision (Eyring et al., 1982) suggests that this may be a general phenomenon in protein-bound isomerizations.

Future resonance Raman studies should provide even more details on how bacterio-opsin and retinal act in concert to produce an efficient light-energy convertor. Important unresolved questions involve the mechanism by which the protein cata-

lyzes deprotonation of the L_{550} intermediate and the mechanism of the thermal conversion of M_{412} back to BR_{568}. Also, it has been shown that under conditions of high ionic strength and/or low light intensity two protons are pumped per photocycle (Kuschmitz & Hess, 1981). How might this be accomplished? Finally, the methods described in this review will also be useful in studies of transduction mechanisms in other retinal-containing pigments, including halorhodopsin, the chloride-ion pump in *H. halobium* (Smith et al., 1984*b*), and rhodopsin, the visual pigment in retinal rod cells (Eyring et al., 1982).

We thank Mark Braiman, Bo Curry and Anne Myers for their contributions to the vibrational analyses summarized here. Johannes A. Pardoen, Albert Broek and Jacques Courtin synthesized the valuable retinal derivatives which were used to perform the isotopic derivative studies. This work was supported by grants from the National Science Foundation (CHE 81-16042) and the National Institutes of Health (EY 02051). Research at Leiden was supported by the Netherlands Foundation of Chemical Research (SON) and by the Netherlands Organization for the Advancement of Pure Research (ZWO). R.M. is an NIH Research Career Development Awardee (EY-00219).

References

Alshuth, T., Stockburger, M. 1981. *Ber. Bunsenges. Phys. Chem.* **85**:484–489

Argade, P.V., Rothschild, K.J. 1983. *Biochemistry* **22**:3460–3466

Aton, B., Doukas, A.G., Callender, R.H., Becher, B., Ebrey, T.G. 1977. *Biochemistry* **16**:2995–2999

Bagley, K., Dollinger, G., Eisenstein, L., Singh, A.K., Zimanyi, L. 1982. *Proc. Natl. Acad. Sci. USA* **79**:4972–4976

Birge, R.R. 1981. *Annu. Rev. Biophys. Bioeng.* **10**:315–354

Birge, R.R., Cooper, T.M. 1983. *Biophys. J.* **42**:61–69

Bogomolni, R., Stubbs, L., Lanyi, J. 1978. *Biochemistry* **17**:1037–1041

Braiman, M. 1983. Ph.D. Thesis. University of California, Berkeley

Braiman, M., Mathies, R. 1982. *Proc. Natl. Acad. Sci. USA* **79**:403–407

Braiman, M., Mathies, R. 1980. *Biochemistry* **19**:5421–5428

Callender, R., Honig, B. 1977. *Annu. Rev. Biophys. Bioeng.* **6**:33–55

Callender, R.H., Doukas, A., Crouch, R., Nakanishi, K. 1976. *Biochemistry* **15**:1621–1629

Curry, B. 1983. Ph.D. Thesis. University of California, Berkeley

Curry, B., Broek, A., Lugtenburg, J., Mathies, R. 1982. *J. Am. Chem. Soc.* **104**:5274–5286

Curry, B., Palings, I., Broek, A., Pardoen, J.A., Mulder, P.P.J., Lugtenburg, J., Mathies, R. 1984. *J. Phys. Chem.* **88**:688–702

El-Sayed, M.A. 1982. *Methods Enzymol.* **88**:617–625

Eyring, G., Curry, B., Mathies, R., Fransen, R., Palings, I., Lugtenburg, J. 1980. *Biochemistry* **19**:2410–2418

Eyring, G., Curry, B., Broek, A., Lugtenburg, J., Mathies, R. 1982. *Biochemistry* **21**:384–393

Hanamoto, J.H., Dupis, P., El-Sayed, M.A. 1984. *Proc. Natl. Acad. Sci. USA* **81**:7083–7087

Harbison, G.S., Herzfeld, J., Griffin, R.G. 1983. *Biochemistry* **22**:1–5

Harbison, G.S., Smith, S.O., Pardoen, J.A., Winkel, C., Lugtenburg, J., Herzfeld, J., Mathies, R., Griffin, R.G. 1984. *Proc. Natl. Acad. Sci. USA* **81**:1706–1709

Henderson, R., Unwin, P.N.T. 1975. *Nature (London)* **257**:28–32

Hess, B., Kuschmitz, D. 1977. *FEBS Lett.* **74**:20–24

Hildebrandt, P., Stockburger, M. 1984. *Biochemistry* **23**:5539–5548

Honig, B., Ebrey, T., Callender, R.H., Dinur, U., Ottolenghi, M. 1979. *Proc. Natl. Acad. Sci. USA* **76**:2503–2507

Hsieh, C-L., Nagumo, M., Nicol, M., El-Sayed, M.A. 1981. *J. Phys. Chem.* **85**:2714–2717

Hsieh, C-L., El-Sayed, M.A., Nicol, M., Nagumo, M., Lee, J-H. 1983. *Photochem. Photobiol.* **38**:83–94

Kakitani, H., Kakitani, T., Rodman, H., Honig, B., Callender, R. 1983. *J. Phys. Chem.* **87**:3620–3628

Khorana, H.G., Gerber, G.E., Herlihy, W.C., Gray, C.P., Anderegg, R.J., Nihei, K., Biemann, K. 1979. *Proc. Natl. Acad. Sci. USA* **76**:5046–5050

Kouyama, T., Kinosita, K., Ikegami, A. 1983. *J. Mol. Biol.* **165**:91–108

Kuschmitz, D., Hess, B. 1981. *Biochemistry* **20**:5950–5957

Lewis, A., Spoonhower, J., Bogomolni, R.A., Lozier, R.H., Stoeckenius, W. 1974. *Proc. Natl. Acad. Sci. USA* **71**:4462–4466

Li, Q.-Q., Govindjee, R., Ebrey, T.G. 1984. *Proc. Natl. Acad. Sci. USA* **81**:7079–7082

Lozier, R.H., Bogomolni, R.A., Stoeckenius, W. 1975. *Biophys. J.* **15**:955–962

Maeda, A., Iwasa, T., Yoshizawa, T. 1977. *J. Biochem.* **82**:1599–1604

Marcus, M.A., Lewis, A. 1978. *Biochemistry* **17**:4722–4735

Massig, G., Stockburger, M., Gartner, W., Oesterhelt, D., Towner, P. 1982. *J. Raman Spectr.* **12**:287–294

Mathies, R. 1979. *Chem. Biochem. Appl. Lasers.* **4**:55–99

Mathies, R., Oseroff, A.R., Stryer, L. 1976. *Proc. Natl. Acad. Sci. USA* **73**:1–5

Myers, A.B., Harris, R.A., Mathies, R.A. 1983. *J. Chem. Phys.* **79**:603–613

Nakanishi, K., Balogh-Nair, V., Arnaboldi, M., Tsujimoto, K., Honig, B. 1980. *J. Am. Chem. Soc.* **102**:7945–7947

Narva, D.L., Callender, R.H., Ebrey, T.G. 1981. *Photochem. Photobiol.* **33**:567–571

Orlandi, G., Schulten, K. 1979. *Chem. Phys. Lett.* **64**:370–374

Oseroff, A.R., Callender, R.H. 1974. *Biochemistry* **13**:4243–4248

Ovchinnikov, Y.A., Abdulaev, N.G., Feigina, M.Y., Kiselev, A.V., Lobanov, N.A. 1979. *FEBS Lett.* **100**:219–224

Pande, J., Callender, R.H., Ebrey, T.G. 1981. *Proc. Natl. Acad. Sci. USA* **78**:7379–7382

Pettei, M.J., Yudd, A.P., Nakanishi, K., Henselman, R., Stoeckenius, W. 1977. *Biochemistry* **16**:1955–1959

Racker, E., Stoeckenius, W. 1974. *J. Biol. Chem.* **249**:662–663

Rothschild, K.J., Argade, P.V., Earnest, T.N., Huang, K.-S., London, E., Liao, M.-J., Bayley, H., Khorana, H.G., Herzfeld, J. 1982. *J. Biol. Chem.* **257**:8592–8595

Rothschild, K.J., Marrero, H. 1982. *Proc. Natl. Acad. Sci. USA* **79**:4045–4049

Rothschild, K.J., Marrero, H., Braiman, M., Mathies, R. 1984*a*. *Photochem. Photobiol.* **40**:675–679

Rothschild, K.J., Roepe, P., Lugtenburg, J., Pardoen, J.A. 1984*b*. *Biochemistry* **23**:6103–6109

Saito, S., Tasumi, M. 1983. *J. Raman Spectr.* **14**:236–245

Schulten, K., Tavan, P. 1978. *Nature (London)* **272:**85–86
Siebert, F., Maentele, W. 1983. *Eur. J. Biochem.* **130:**565–573
Slifkin, M.A., Caplan, S.R. 1975. *Nature (London)* **253:**56–58
Smith, S.O. 1985. Ph.D. Thesis. University of California, Berkeley
Smith, S.O., Braiman, M., Mathies, R. 1983*b*. *In:* Time-Resolved Vibrational Spectroscopy. G.H. Atkinson, editor. pp. 219–230. Academic, New York
Smith, S.O., Marvin, M.J., Bogomolni, R.A., Mathies, R. 1984*b*. *J. Biol. Chem.* **259:**12326–12329
Smith, S.O., Myers, A.B., Pardoen, J.A., Winkel, C., Mulder, P.P.J., Lugtenburg, J., Mathies, R. 1984*a*. *Proc. Natl. Acad. Sci. USA* **81:**2055–2059
Smith, S.O., Myers, A.B., Mathies, R.A., Pardoen, J.A., Winkel, C., Berg, E.M.M. van den, Lugtenburg, J. 1985. *Biophys. J. (in press)*
Smith, S.O., Pardoen, J.A., Mulder, P.P.J., Curry, B., Lugtenburg, J., Mathies, R. 1983*a*. *Biochemistry* **22:**6141–6148
Sperling, W., Carl, P., Rafferty, C.N., Dencher, N. 1977. *Biophys. Struct. Mechan.* **3:**79–94
Stockburger, M., Klusmann, W., Gattermann, H., Massig, G., Peters, R. 1979. *Biochemistry* **18:**4886–4900
Stoeckenius, W., Bogomolni, R.A. 1982. *Annu. Rev. Biochem.* **51:**587–616
Terner, J., Campion, A., El-Sayed, M.A. 1977. *Proc. Natl. Acad. Sci. USA* **74:**5212–5216
Terner, J., Hsieh, C.-L., Burns, A.R., El-Sayed, M.A. 1979*a*. *Biochemistry* **18:**3629–3634
Terner, J., Hsieh, C.-L., El-Sayed, M.A. 1979*b*. *Biophys. J.* **26:**527–541
Terner, J., Hsieh, C.-L., Burns, A.R., El-Sayed, M.A. 1979*c*. *Proc. Natl. Acad. Sci. USA* **76:**3046–3050
Tsuda, M., Glaccum, M., Nelson, B., Ebrey, T.G. 1980. *Nature (London)* **287:**351–353
Warshel, A. 1977. *Annu. Rev. Biophys. Bioeng.* **6:**273–300
Warshel, A. 1979. *Photochem. Photobiol.* **30:**285–290
Warshel, A., Barboy, N. 1982. *J. Am. Chem. Soc.* **104:**1469–1476

Received 6 December 1984; revised 11 February 1985